

NISTIR 4670

**Electronics and Electrical
Engineering Laboratory**

Technical Progress Bulletin

Covering Laboratory Programs,
April to June 1991,
with 1992 EEEL Events Calendar

**U.S. DEPARTMENT OF COMMERCE
National Institute of Standards
and Technology
Electronics and Electrical
Engineering Laboratory
Semiconductor Electronics Division
Gaithersburg, MD 20899**

October 1991

91-2

**U.S. DEPARTMENT OF COMMERCE
Robert A. Mosbacher, Secretary
NATIONAL INSTITUTE OF STANDARDS
AND TECHNOLOGY
John W. Lyons, Director**

NIST

NISTIR 4670

**Electronics and Electrical
Engineering Laboratory**

Technical Progress Bulletin

Covering Laboratory Programs,
April to June 1991,
with 1992 EEEL Events Calendar

**U.S. DEPARTMENT OF COMMERCE
National Institute of Standards
and Technology
Electronics and Electrical
Engineering Laboratory
Semiconductor Electronics Division
Gaithersburg, MD 20899**

October 1991

91-2



**U.S. DEPARTMENT OF COMMERCE
Robert A. Mosbacher, Secretary
NATIONAL INSTITUTE OF STANDARDS
AND TECHNOLOGY
John W. Lyons, Director**

INTRODUCTION TO OCTOBER 1991 ISSUE OF THE EEEL TECHNICAL PROGRESS BULLETIN

This is the thirty-fifth issue of a quarterly publication providing information on the technical work of the National Institute of Standards and Technology Electronics and Electrical Engineering Laboratory (EEEL, until February 1991, the Center for Electronics and Electrical Engineering). This issue of the EEEL Technical Progress Bulletin covers the second quarter of calendar year 1991.

Organization of Bulletin: This issue contains abstracts for all relevant papers released for publication by NIST in the quarter and citations and abstracts for such papers published in the quarter. Entries are arranged by technical topic as identified in the Table of Contents and alphabetically by first author under each subheading within each topic. Unpublished papers appear under the subheading "Released for Publication." Papers published in the quarter appear under the subheading "Recently Published." Following each abstract is the name and telephone number of the individual to contact for more information on the topic (usually the first author). This issue also includes a calendar of Laboratory conferences and workshops planned for calendar year 1992 and a list of sponsors of the work.

Electronics and Electrical Engineering Laboratory: EEEL programs provide national reference standards, measurement methods, supporting theory and data, and traceability to national standards. The metrological products of these programs aid economic growth by promoting equity and efficiency in the marketplace, by removing metrological barriers to improved productivity and innovation, by increasing U.S. competitiveness in international markets through facilitation of compliance with international agreements, and by providing technical bases for the development of voluntary standards for domestic and international trade. These metrological products also aid in the development of rational regulatory policy and promote efficient functioning of technical programs of the Government.

The work of the Laboratory is conducted by four technical research Divisions: the Semiconductor Electronics and the Electricity Divisions in Gaithersburg, Md., and the Electromagnetic Fields and Electromagnetic Technology Divisions in Boulder, Colo. In 1991, the Office of Law Enforcement Standards, formerly the Law Enforcement Standards Laboratory, was transferred to EEEL. This Office conducts research and provides technical services to the U.S. Department of Justice, State and local governments, and other agencies in support of law enforcement activities. In addition, the Office of Microelectronics Programs (OMP) was established in EEEL to coordinate the growing number of semiconductor-related research activities at NIST. Reports of work funded through the OMP are included under the heading "Semiconductor Microelectronics."

Key contacts in the Laboratory are given on the back cover; readers are encouraged to contact any of these individuals for further information. To request a subscription or for more information on the Bulletin, write to EEEL Technical Progress Bulletin, National Institute of Standards and Technology, Metrology Building Room B-358, Gaithersburg, MD 20899 or call (301) 975-2220.

Laboratory Sponsors: The Laboratory Programs are sponsored by the National Institute of Standards and Technology and a number of other organizations, in both the Federal and private sectors; these are identified on page 30.

Note on Publication Lists: Publication lists covering the work of each division are guides to earlier as well as recent work. These lists are revised and reissued on an approximately annual basis and are available from the originating division. The current set is identified in the Additional Information section, page 28.

TABLE OF CONTENTS

INTRODUCTION	inside title page
FUNDAMENTAL ELECTRICAL MEASUREMENTS	2
SEMICONDUCTOR MICROELECTRONICS	2
Silicon Materials	3
Compound Materials	3
Analysis Techniques	4
Device Physics and Modeling	4
Insulators and Interfaces	6
Dimensional Metrology	8
Integrated Circuit Test Structures	8
Microfabrication Technology	10
Plasma Processing	12
Power Devices	12
Photodetectors	12
Reliability	13
SIGNAL ACQUISITION, PROCESSING, & TRANSMISSION	13
DC & Low Frequency Metrology	13
Waveform Metrology	15
Cryoelectronic Metrology	16
Antenna Metrology	17
Noise Metrology	17
Microwave & Millimeter-Wave Metrology	18
Electromagnetic Properties	20
Optical Fiber Metrology	21
Optical Fiber Sensors	21
Electro-Optic Metrology	22
Other Signal Metrology Topics	22
ELECTRICAL SYSTEMS	23
Power Systems Metrology	23
Magnetic Materials & Measurements	25
Superconductors	26
Other Electrical Systems Topics	27
ELECTROMAGNETIC INTERFERENCE	27
Conducted	27
Radiated	27
ADDITIONAL INFORMATION	28
1992 EEEL CALENDAR	29
EEEL SPONSOR	30
KEY CONTACTS IN LABORATORY, LABORATORY ORGANIZATION	inside back cover

FUNDAMENTAL ELECTRICAL MEASUREMENTS

Recently Published

Cage, M.E., Yu, D., Jeckelmann, B.M., Steiner, R.L., and Duncan, R.V., **Investigating the Use of Multimeters to Measure Quantized Hall Resistance Standards**, IEEE Transactions on Instrumentation and Measurement (Special Issue of selected papers, CPEM '90), Vol. 40, No. 2, pp. 262-266 (April 1991). [Also published in the Digest of the 1990 Conference on Precision Electromagnetic Measurements, Ottawa, Canada, June 11-14, 1990, pp. 332-333 (1990).]

A new generation of digital multimeters was used to directly compare the ratios of the resistances of wire-wound reference resistors and quantized Hall resistances. The accuracies are better than 0.1 parts per million for ratios as large as 4:1 if the multimeters are calibrated with a Josephson array.

[Contact: Marvin E. Cage, (301) 975-4249]

Kinoshita, J., Nishinaka, H., Segawa, K., Van Degrift, C.T., and Endo, T., **Measurements of the Quantized Hall Resistance at ETL**, IEEE Transactions on Instrumentation and Measurement, Vol. 40, No. 2, pp. 249-252 (April 1991).

The quantized Hall resistance $R_H(4)$ for Si-MOSFETs and a GaAs heterostructure device has been measured in terms of Ω_{ETL} by use of a newly constructed measurement system at the Electrotechnical Laboratory (ETL), Tsukuba, Ibaraki, 305 Japan. The result is $R_H(4) = 6453.1992 \pm 0.0002 \Omega_{ETL} = 6543.20175(1 - 0.40 \times 10^{-6} \pm 0.03 \times 10^{-6}) \Omega_{ETL}$ on January 1, 1990.

[Contact: Craig T. Van Degrift, (301) 975-4249]

Released for Publication

Steiner, R., and Stahley, S., **MAP Voltage Transfer Between 10-V Josephson Array Systems**, to be published in the Proceedings of the 1991 National Conference of Standards Laboratories Workshop and Symposium, Albuquerque, New Mexico, August 19-22, 1991.

A Measurement Assurance Program (MAP) for voltage transfer at the 10-V level was performed among six U.S. laboratories currently operating 10-V Josephson array systems. A commercial voltage standard based on four Zener references was used as the transfer device. This experiment provided data on the precision and traceable

accuracy of the various array systems relative to the national Si-volt representation at the National Institute of Standards and Technology (NIST), as well as on calibrations involving the new multi-Zener reference standards. Preliminary measurements from five other laboratories show that all agree with NIST to within 0.035 parts per million with a maximum random uncertainty of 0.015 parts per million (1σ).

[Contact: Richard Steiner, (301) 975-4226]

Yoshihiro, K., Van Degrift, C.T., Cage, M.E., and Yu, D., **Anomalous Behavior of a Quantized Hall Plateau in a High-Mobility Si-MOSFET**.

Measurements at 14 T and 340 mK of the $i=4$ quantized Hall resistances of a Si-MOSFET made with a precision of 0.005 parts per million and an accuracy of 0.015 parts per million revealed unexpected irregularities. Smooth variations of ± 0.04 parts per million were observed across the plateau even though the Si-MOSFET had a mobility of $1.2 \text{ m}^2/\text{V}\cdot\text{s}$ and a longitudinal resistivity less than 0.002 parts per million of the plateau resistivity. Furthermore, measurements over a period of several months indicated that the plateau shape is metastable. A variety of possible causes for these phenomena are discussed, but none provides a satisfactory explanation.

[Contact: Craig T. Van Degrift, (301) 975-4248]

SEMICONDUCTOR MICROELECTRONICS

Recently Published

Oettinger, F.F., **NIST Semiconductor Electronics Division Works to Assist U.S. Industry**, SRC Newsletter, Vol. 9, No. 3, pp. 1-4 (March 1991).

Within the Electronics and Electrical Engineering Laboratory at NIST is the Semiconductor Electronics Division. For more than 30 years, the Division has maintained a tradition of improving manufacturing productivity and aiding in the development, transfer, and application of semiconductor technology. Activities of the Division include basic investigation of the theory and behavior of materials and structures, improvement of measurement methods to characterize materials and devices, development of metrology and artifacts for the manufacture of integrated circuits, and the creation of special circuits used in characterizing the performance of transistors. Two specific projects, X-ray lithography and electromigration, are described in detail.

[Contact: Frank F. Oettinger, (301) 975-2054]

Silicon Materials

Recently Published

Richter, M., Woicik, J.C., Nogami, J., Pianetta, P., Miyano, K.E., Baski, A.A., Kendelewicz, T., Bouldin, C.E., Spicer, W.E., Quate, C.F., and Lindau, I., **Surface Extended-X-Ray-Absorption Fine Structure and Scanning Tunneling Microscopy of Si(001) 2×1 -Sb**, Physical Review Letters, Vol. 65, No. 27, pp. 3417-3420 (31 December 1990).

Scanning tunnelling microscopy (STM) has been combined with surface extended X-ray adsorption fine structure (SEXAFS) to determine both the local and long-range bonding properties of the Si(001) 2×1 -Sb surface. Phase and amplitude analysis of the Sb L_3 edge SEXAFS shows that the Sb atoms occupy a modified bridge site and form dimers on the Si(001) surface with a Sb-Sb near-neighbor distance of $2.88 \pm 0.03 \text{ \AA}$. Each Sb atom of the dimer is bonded to two Si atoms with a Sb-Si bond length of $2.63 \pm 0.04 \text{ \AA}$. STM resolves the dimer structure and provides the long-range periodicity of the surface. Low-energy electron diffraction of vicinal Si(001) shows that the Sb dimer chains run perpendicular to the Si dimer chains.

[Contact: David G. Seiler, (301) 975-2081]

Roitman, P., Simons, D.S., Chi, P.H., Lindstron, R.M., Lux, G.E., Baumann, S., Novak, S.W., Wilson, R.G., Farrington, D., Keenan, J., Stevie, F.A., Moore, J.L., Irwin, R.B., Filo, A.J., Magee, C.W., Alcorn, R., and File, D., **Round-Robin Study of Implants in Si and SiO₂ by SIMS, RBS, and NAA**, Proceedings of the Seventh International Conference on Secondary Ion Mass Spectrometry (SIMS VII), Monterey, California, September 3-8, 1989, pp. 115-117 (1990).

A round-robin study of implants of C, Na, Al, Cr, Fe, and Cu into Si and SiO₂ has been conducted. The results are reported.

[Contact: Peter Roitman, (301) 975-2077]

Compound Materials

Recently Published

McKeown, D.A., **XANES of Transition Metal Zinc-Blende Semiconductors**, X-ray Absorption Fine Structure, Chapter 85, pp. 346-348 (Ellis Horwood Limited, Eds., 1991). (Proceedings of the Sixth International Conference on X-ray Absorption Fine Structure, York, United Kingdom, August 5-11, 1990.)

XANES (X-ray absorption near-edge structure) is known to be sensitive to both the arrangement of atoms around, as well as the atomic states of, the absorbing atom. Therefore, it is not surprising that XANES data, collected on compounds having different arrangements of atoms around the absorbing atom, can have very different features. In this study, XANES data were gathered for three transition metals: Fe and Cu in chalcopyrite (CuFeS₂), and Zn in sphalerite (ZnS), where all three cations are in nearly identical atomic environments (similar to the zinc-blende type structures in III-V semiconductors). Since the environments are similar, any change in the XANES should, to first approximation, be due entirely to atomic effects of the absorbing atom. The rationale behind this study is to see if any changes in the near-edge data can be assigned to electronic transitions of the absorbing atom; this may be useful for interpreting XANES for III-V semiconductors. Previously, Zn, Cu, and Fe edges were presented separately, but no comparisons or calculations have been made for all three edges.

[Contact: David A. McKeown, (301) 975-3095]

Seiler, D.G., Lowney, J.R., Littler, C.L., and Yoon, I.T., **Intrinsic Carrier Concentrations in Long Wavelength HgCdTe Based on the New, Nonlinear Temperature Dependence of $E_g(x,T)$** , Proceedings of the Materials Research Society Symposium, Boston, Massachusetts, November 26-29, 1990, Vol. 216, pp. 59-63 (1991).

Intrinsic carrier concentrations of narrow-gap Hg_{1-x}Cd_xTe alloys ($0.17 \leq x \leq 0.30$) have been calculated as a function of temperature between 0 and 300 K by using the new nonlinear temperature dependence of the energy gap obtained previously by two-photon magneto-absorption measurements for samples with $0.24 \leq x \leq 0.26$. We report here experimental values for $E_g(x,T)$ for samples with $x = 0.20$ and 0.23 obtained by one-photon magneto-absorption measurements. These data confirm the validity of the new $E_g(x,T)$ relationship for these x values. In this range of composition and temperature, the energy gap of mercury cadmium telluride is small, and very accurate values are needed for the gap to obtain reliable values for the intrinsic carrier density. Large percentage differences exist between new calculations and previous values for n_i at low temperatures. Even at 77 K, differences approaching 10% exist, confirming the importance of using the new n_i results for materials and device characterization and a proper understanding of device operation in long-wavelength materials.

[Contact: David G. Seiler, (301) 975-2081]

Released for Publication

Huang, D., Kallergi, M., Aubel, J., Sundaram, S., DeSalvo, G.C., and Comas, J., **Lattice Damage and Atomic Mixing Induced by As⁺⁺ Implantation and Thermal Annealing in AlAs/GaAs Multiple Quantum Well Structures.**

The lattice damage and the nature of the atomic intermixing of Al and Ga induced by As⁺⁺ implantation and thermal annealing in AlAs/GaAs multiple quantum-well structures were investigated. The photoluminescence spectra, which show multiple peaks after implantation and annealing, were analyzed based on the shifts of the excitonic peaks arising from quantum wells located at different depths. The depth profiles of intermixing were obtained using a procedure of successive layer-by-layer chemical etching following photoluminescence measurements. It is found that the mixing is maximum near the sample surface and decreases monotonically with depth, suggesting that the profiles follow the ion-induced damage more closely than the ion density. It is also observed that the damage extends beyond 1 μm . Within 0.3 μm from the surface, the damage is heavy and the atomic intermixing increases rapidly with ion dose, indicating the damage is structural. Beyond 0.3 μm , the degree of intermixing is only sensitive to the anneal temperature but not to the implantation dose. The results show that both direct collisions and interdiffusion are responsible for the atomic mixing. For the samples implanted with ion doses below 10^{14} $1/\text{cm}^2$ and annealed at 650 $^\circ\text{C}$, the optical activation from radiation damage is appreciable. However, the interdiffusion becomes important at temperatures near and above 800 $^\circ\text{C}$.

[Contact: Gregory C. DeSalvo, (301) 975-2431]

Lowney, J.R., Seiler, D.G., Littler, C.L., and Yoon, I.T., **Intrinsic Carrier Concentration of Narrow-Gap Mercury Cadmium Telluride Based on the Nonlinear Temperature Dependence of the Bandgap.**

The intrinsic carrier concentrations of narrow-gap alloys of $\text{Hg}_{1-x}\text{Cd}_x\text{Te}$ have been calculated as a function of temperature between 0 and 300 K for x -values between 0.17 and 0.30. The new and more accurate relation for the temperature dependence of the energy gap, which is based on two-photon magnetoabsorption data, is used. This relation is further supported here by additional one-photon magnetoabsorption measurements for $x = 0.20$ and 0.23 , which were made with a CO_2 laser. In this range of composition and temperature, the energy gap of mercury cadmium telluride is small, and very

accurate values are needed for the gap to obtain reliable values for the intrinsic carrier density. Kane's $k \cdot p$ theory is used to account for the conduction-band nonparabolicity. Large percentage differences occur between new calculations and previously calculated values for n_i at low temperatures. A nonlinear least-squares fit was made to the results of these calculations for ease of use. The implications of these results for $\text{Hg}_{1-x}\text{Cd}_x\text{Te}$ materials characterization and device operation are discussed.

[Contact: Jeremiah R. Lowney, (301) 975-2048]

Analysis Techniques

Recently Published

Kopanski, J.J., Carver, G.P., Lowney, J.R., Miles, D.S., and Novotny, D.B., **High Spatial Resolution Mapping of Semiconductor Resistivity**, Extended Abstract, Electrochemical Society Spring Meeting, Washington, D.C., May 5-10, 1991, Vol. 91-1, pp. 698-699 (1991).

A new approach to the resistivity mapping of semiconductors uses an array of lithographically defined contacts (at a density of 60,000 sites per cm^2) and an automated probe station for data acquisition. Resistivity growth striations in silicon as narrow as 45 μm^2 in width and with $\pm 5\%$ variation from the background resistivity have been resolved. Solution of the Laplace equation for the measurement geometry and measurements on ion-implanted test structures are described. Anticipated applications include resistivity mapping of liquid-encapsulated Czochralski GaAs, $\text{Hg}_{1-x}\text{Cd}_x\text{Te}$, and fine-scale resistivity variations in processed silicon.

[Contact: Joseph J. Kopanski, (301) 975-2089]

Device Physics and Modeling

Recently Published

Hefner, A.R., Jr., **Device Models, Circuit Simulation, and Computer Controlled Measurements for the IGBT**, Proceedings of the 1990 IEEE Workshop on Computers in Power Electronics, Lewisburg, Pennsylvania, August 22-23, 1990, pp. 233-243 (1991).

The implementation of the recently developed IGBT device model into a circuit simulation program is described. It is shown that the circuit simulation program rapidly and robustly simulates the dynamic behavior of the IGBT for general external drive, load,

and feedback circuit configurations. The algorithms used to extract the IGBT device parameters from computer-controlled measurements are also described, and it is shown that the model gives accurate results when the extracted parameters are used.

[Contact: Allen R. Hefner, Jr., (301) 975-2071]

Hefner, A.R., Jr., **An Investigation of the Drive Circuit Requirements for the Power Insulated Gate Bipolar Transistor (IGBT)**, IEEE Transactions on Power Electronics, Vol. 6, No. 2, pp. 208-219 (April 1991). [Also published in the Conference Record, 21st Annual Power Electronics Specialists Conference (PESC '90), San Antonio, Texas, June 10-15, 1990, pp. 126-137 (June 1990).]

The drive circuit requirements of the IGBT are explained with the aid of an analytical model. It is shown that non-quasi-static effects limit the influence of the drive circuit on the time rate-of-change of anode voltage. Model results are compared with measured turn-on and turn-off waveforms for different drive circuits, load circuits, and different IGBT base lifetimes. [Contact: Allen R. Hefner, Jr., (301) 975-2071]

Lowney, J.R., and Bennett, H.S., **Majority and Minority Electron and Hole Mobilities in Heavily Doped GaAs**, Journal of Applied Physics, Vol. 69, No. 10, pp. 7102-7110 (15 May 1991).

The majority electron and minority hole mobilities have been calculated in GaAs for donor densities between 5×10^{16} and $1 \times 10^{19} \text{ cm}^{-3}$. Similarly, the majority hole and minority electron mobilities have been calculated for acceptor densities between 5×10^{16} and $1 \times 10^{20} \text{ cm}^{-3}$. All the important scattering mechanisms have been included. The ionized impurity and carrier-carrier scattering processes have been treated with a phase-shift analysis. These calculations are the first to use a phase-shift analysis for minority carriers scattering from majority carriers. The results are in good agreement with experiment, but predict that at high dopant densities, minority mobilities should increase with increasing dopant density for a short range of densities. This effect occurs because of the reduction of plasmon scattering and the removal of carriers from carrier-carrier scattering because of the Pauli exclusion principle. Some recent experiments support this finding. These results are important for device modeling because of the need to have values for the minority mobilities and the difficulty in measuring them.

[Contact: Jeremiah R. Lowney, (301) 975-2048]

Myers, D.R., Lott, J.A., Lowney, J.R., Klem, J.F., and Tigges, C.P., **Band-Gap Narrowing and III-V Heterostructure FETs**, IEDM Technical Digest, International Electron Devices Meeting 1990, San Francisco, California, December 9-12, 1990, pp. 31.1.1-31.1.4 (1990).

We calculate the magnitude of band-gap narrowing for GaAs-based alloys, and have included these results into one-dimensional heterojunction device models for strained $\text{In}_{0.15}\text{Ga}_{0.85}\text{As}$ quantum-well MODulation-doped Field-Effect Transistors (MODFETs). Equivalent rigid shifts of as much as 102 meV are obtained for the valence band of depleted p-type $\text{Al}_{0.15}\text{Ga}_{0.85}\text{As}$ doped at $5 \times 10^{18}/\text{cm}^3$. Our simulations suggest that band-gap narrowing is most significant for p-channel MODFETs. The predicted effect of band-gap narrowing in p-channel MODFETs is the formation of parasitic conduction in the low-mobility parent dopant region. The parasitic conduction would reduce the intrinsic gain.

[Contact: Jeremiah R. Lowney, (301) 975-2048]

Released for Publication

Hefner, A.R., Jr., and Diebolt, D.M., **An Experimentally Verified IGBT Model Implemented in the Saber Circuit Simulator**, to be published in the Proceedings of the Power Electronics Specialist Conference, Cambridge, Massachusetts, June 24-27, 1991.

A physics-based Insulated Gate Bipolar Transistor (IGBT) model is implemented into the general purpose circuit simulator Saber. The IGBT model includes all of the physical effects that have been shown to be important for describing IGBTs, and the model is valid for general external circuit conditions. The Saber IGBT model is evaluated for the range of static and dynamic conditions in which the device is intended to be operated, and the simulations compare well with experimental results for all of the conditions studied.

[Contact: Allen R. Hefner, Jr., (301) 975-2071]

Korman, C.E., Mayergoyz, I.D., and Gaitan, M., **Numerical Simulation of Quasi-Stationary Effects in Thin-Film SOI MOSFETs**.

A new finite-difference iterative method has been developed to simulate SOI (silicon-on-insulator) MOSFETs in the steady-state and quasi-stationary regimes. The simulations are used to study an effective threshold voltage shift and drain current overshoot caused by a stagnant majority carrier distribution. It is

shown that this effect is minimized by using fully depleted (thin) silicon layers. The quasi-stationary solution assumes a stagnant majority carrier distribution in the silicon film due to isolation from the bulk by an insulating layer. The quasi-stationary solution simulates the device immediately after an abrupt change in the gate bias since the time to restore the majority carriers to steady state is limited by the finite generation/recombination time. When this approximation is used, the more involved full transient simulation is avoided.

[Contact: Michael Gaitan, (301) 975-2070]

Mitter, C.S., Hefner, A.R., Jr., Chen, D.Y., and Lee, F.C., **Insulated Gate Bipolar Transistor (IGBT) Modeling Using IG-Spice**, to be published in the Proceedings of the IEEE Industry Applications Society 1991 Meeting, Dearborn, Michigan, September 29-October 4, 1991.

A physics-based model for the Insulated Gate Bipolar Transistor (IGBT) is implemented into the widely available circuit simulation package IG-Spice. Based on analytical equations describing the semiconductor-physics, the model accurately describes the nonlinear junction capacitances, moving boundaries, recombination, and carrier scattering, and effectively predicts the device conductivity modulation. In this paper, the procedure used to incorporate the model into IG-Spice and various methods necessary to ensure convergence are described. The effectiveness of the Spice-based IGBT model is demonstrated by investigating the static and dynamic current sharing of paralleled IGBTs with different device model parameters. The simulated results are verified by comparison with experimental results.

[Contact: Allen R. Hefner, Jr., (301) 975-2071]

Insulators and Interfaces

Recently Published

Chandler-Horowitz, D., Marchiando, J.F., Doss, M., Krause, S., and Visitserntrakul, S., **Sensitivity of Ellipsometric Modeling to the "Islands" of Silicon Precipitates at the Bottom of the Buried Oxide Layer in Annealed SIMOX**, Technical Abstract, 1990 IEEE SOS/SOI Technology Conference, Key West, Florida, October 2-4, 1990, pp. 73-74 (1990).

Spectroscopic ellipsometry is a nondestructive probe which can be highly sensitive to the multilayer structure of materials such as SIMOX. Recent TEM micrographs of high-flux single-implant SIMOX annealed at 1300 °C

for 6 h show "islands" of silicon precipitates near the bottom of the buried oxide layer. Spectroscopic ellipsometric measurements were performed on these samples at various implant doses and beam current densities to observe how the measured data fit the data theoretically predicted for various models of SIMOX that lead to the presence of these "islands."

[Contact: Deane Chandler-Horowitz, (301) 975-2084]

Chandler-Horowitz, D., Marchiando, J.F., and Belzer, B.J., **Ellipsometry SRM's for Use in Thin Film Measurements**, Proceedings of the Measurement Science Conference (MSC), Anaheim, California, February 8-9, 1990, pp. 5A-11 to 5A-21 (1990).

A Standard Reference Material (SRM) consisting of a film of silicon dioxide on a silicon substrate has been designed, fabricated, measured, and certified at the National Institute of Standards and Technology for the ellipsometric angles, Δ and ψ , and for the derived film thickness and refractive index. This SRM can be used as an aid in the evaluation of the performance of optical and mechanical thickness-monitoring instruments as well as ellipsometers. The optical instruments are based on the theory describing reflection of light from a sample. The film thickness is determined by using a model having one or two uniform isotropic films atop a substrate. The calculated thicknesses rely on accurate values of the indices of refraction of the substrate and/or film at the necessary wavelengths. The measurement procedure used here to certify the ellipsometric angles utilizes an accurate rotating-analyzer ellipsometer and HeNe laser source operating near the principal angle of incidence. The measurement data from several samples are analyzed collectively to determine the certified film thicknesses and refractive index. At the present time, three different film thicknesses, 50, 100, and 200 nm, are being certified. Future work may involve certifying thinner layers of oxides.

[Contact: Deane Chandler-Horowitz, (301) 975-2084]

Chi, P.H., Simons, D.S., and Roitman, P., **Quantitative Analysis of Impurities in SIMOX Samples using Secondary Ion Mass Spectrometry**, Surface and Interface Analysis, Vol. 17, pp. 57-61 (1991).

Silicon films produced by the SIMOX process (separation by implanted oxygen) must be annealed at high temperature to remove the crystal damage introduced during implantation of the high oxygen dose. Different annealing gases, temperatures, and times have been investigated. In such processes, various impurities

present in the high-temperature ceramic furnace tube, as well as annealing gas species, may be incorporated into the samples. Secondary ion mass spectrometry (SIMS) is used as a quantitative tool to analyze the diffusion of tube components and gases into annealed SIMOX samples. Samples prepared for this investigation were annealed in nitrogen and argon at temperatures ranging from 1250 to 1350 °C. It was found that most impurities are present at low levels and are generally trapped in the surface oxide that is grown during the anneal. SIMS analyses of SIMOX samples annealed in nitrogen showed that nitrogen tends to collect in both the surface oxide and buried oxide layers, piling up at the oxide/silicon interfaces.

[Contact: Peter Roitman, (301) 975-2077]

Kopanski, J.J., Carver, G.P., Lowney, J.R., Miles, D.S., and Novotny, D.B., **High Spatial Resolution Mapping of Semiconductor Resistivity**, Extended Abstract, Electrochemical Society Spring Meeting, Washington, D.C., May 5-10, 1991, Vol. 91-1, pp. 698-699 (1991).

A new approach to the resistivity mapping of semiconductors uses an array of lithographically defined contacts (at a density of 60,000 sites per cm^2) and an automated probe station for data acquisition. Resistivity growth striations in silicon as narrow as 45 μm in width and with $\pm 5\%$ variation from the background resistivity have been resolved. Solution of the Laplace equation for the measurement geometry and measurements on ion-implanted test structures are described. Anticipated applications include resistivity mapping of liquid-encapsulated Czochralski GaAs, $\text{Hg}_{1-x}\text{Cd}_x\text{Te}$, and fine-scale resistivity variations in processed silicon.

[Contact: Joseph J. Kopanski, (301) 975-2089]

Mayo, S., Lowney, J.R., Roitman, P., and Novotny, D.B., **Persistent Photoconductivity in SIMOX Films**, Technical Abstract, 1990 IEEE SOS/SOI Technology Conference, Key West, Florida, October 2-4, 1990, pp. 156-157 (1990).

Photoinduced transient spectroscopy (PITS) was used to measure the persistent photoconductive (PPC) response in film resistors fabricated on two different commercial n-type SIMOX (separation by implanted oxygen) wafers. A broadband, single-shot, flashlamp-pumped dye laser pulse was used to photoexcite interband electrons in the film, and the decay in the induced excess carrier population was measured at temperatures in the 60- to 220-K range. The post-illumination conductivity transients observed show PPC signals exhibiting

nonexponential character. They were recorded for periods of time up to 30 s at constant temperature. The photoconductive data from these film resistors are analyzed by using the Queisser and Theodorou potential barrier model, and a logarithmic time decay dependence is confirmed for the first time in SIMOX material. The sensitivity of PITS is demonstrated to be appropriate for characterization of the SIMOX interface structure and for material qualification.

[Contact: Santos Mayo, (301) 975-2045]

Roitman, P., Edelstein, M., Krause, S., and Visitserntrukul, S., **Residual Defects in SIMOX: Threading Dislocations and Pipes**, Technical Abstract, 1990 IEEE SOS/SOI Technology Conference, Key West, Florida, October 2-4, 1990, pp. 154-155 (1990).

In the past few years, due to improved control of the ion implantation process and improved annealing sequences, a qualitative improvement has been realized in the structural quality of SIMOX films. The dense network of oxide precipitates and threading dislocations in the top silicon can be annealed out, reducing the dislocation density from $\approx 10^{10}/\text{cm}^2$ to $\approx 10^5/\text{cm}^2$ or less. CMOS transistors and circuits have been successfully fabricated in this material. However, bipolar devices are sensitive to defect densities in this range, as is VLSI yield. Therefore, the defect density must be monitored and reduced. We discuss below some techniques for monitoring dislocations and stacking faults in SIMOX films. Also, a different type of defect, a silicon "pipe" running through the buried oxide, has been observed. The origin of these defects and a technique for detecting them are described.

[Contact: Peter Roitman, (301) 975-2077]

Released for Publication

Mayo, S., Lowney, J.R., and Roitman, P., **Measurement of Interface Defects in Gated SIMOX Structures**, to be published in the Proceedings of the 1991 IEEE International SOI Conference, Vail Valley, Colorado, October 1-3, 1991.

Defects in gated or ungated thin film resistors have been characterized by photoinduced transient spectroscopy (PITS). The resistors were fabricated with n- or p-type SIMOX (separation by implanted oxygen) wafers implanted with 200-keV oxygen to $1.8 \times 10^{18} \text{ cm}^{-2}$ total fluence. One wafer used for gated resistor fabrication was implanted at 595 °C and sequentially annealed at 1325 °C for 4 h in argon (plus 0.5% oxygen) followed by 4 h in nitrogen (plus 0.5% oxygen). Another wafer

used for ungated resistor fabrication was implanted at 650 °C and annealed at 1275 °C for 2 h in nitrogen (plus 0.5% oxygen). PITS data indicate that electron or hole traps in the conductive silicon film are located at the film-buried silica interface. We estimate the average interface trap density in the SIMOX structure to be in the 10^{11} cm⁻² range.

[Contact: Santos Mayo, (301) 975-2045]

Dimensional Metrology

Recently Published

Postek, M.T., Larrabee, R.D., Keery, W.J., and Marx, E., **The Application of Transmission Electron Detection to X-ray Mask Calibrations and Inspection**, Proceedings of SPIE (The International Society for Optical Engineering, P.O. Box 10, Bellingham, Washington 98227-0010), Integrated Circuit Metrology, Inspection, and Process Control V, Vol. 1464, pp. 35-47 (1991).

Masks used for the manufacture of integrated circuits by X-ray lithography can be calibrated and inspected in a scanning electron microscope by using the transmitted electron detection mode. By their nature, these masks present a measurement subject unique from most (if not all) other objects used in semiconductor processing because the support membrane is, by design, X-ray transparent. This characteristic can be used as an advantage in electron beam-based mask metrology since, depending upon the incident electron beam voltages, substrate composition and substrate thickness, the membrane can also be essentially electron transparent. The areas of the mask where the absorber structures are located are essentially X-ray opaque as well as electron opaque. Viewing the sample from a perspective below an X-ray mask can provide excellent electron signal contrast (depending upon the instrument conditions) between the absorber structure and the membrane. Thus, the mask can be viewed in the transmitted electron detection mode of the scanning electron microscope, and precise and potentially accurate dimensional measurements can be made. One unique advantage to this is that in the transmitted electron detection mode, the modeling of the electron beam/specimen interaction becomes far less difficult than in the modeling of typical secondary electron images of opaque objects. The inelastically scattered beam electrons and the low-energy secondary electrons can be excluded from the detector and, therefore, need not be accurately modeled. Therefore, absorber structure width (linewidth) measurement standards can

be potentially calibrated with less difficulty and higher accuracy than standards calibrated by more conventional means. The transmitted electron detection mode is also useful, because of the high contrast of the image, for the determination of mask defects and high-density particle detection as well as for registration measurements.

[Contact: Michael T. Postek, (301) 975-2299]

Integrated Circuit Test Structures

Recently Published

Cresswell, M.W., Gaitan, M., Allen, R.A., and Linholm, L.W., **A Modified Sliding Wire Potentiometer Test Structure for Mapping Nanometer-Level Distances**, Proceedings of the IEEE 1991 International Conference on Microelectronic Test Structures, Kyoto, Japan, March 18-20, 1991, Vol. 4, No. 1, pp. 129-134 (1991).

This paper presents a modified voltage-dividing potentiometer test structure which overcomes a problem typical in scaling electrical test structures; it provides a correction for electrical length shortening of a resistor strip caused by the attachment of voltage taps of non-negligible width. The test structure was implemented in chrome on quartz, and measurements of displacements between 10 and 500 nm with ± 12 -nm random error were made using available test equipment. The enhanced precision of the measurement derives from reducing the size of the structure from previous design methods. The enhanced accuracy of the displacement measurement derives from scaling the length of the potentiometer bridge while simultaneously providing for non-scaled widths of the voltage taps. Measurements using these corrections demonstrate an improvement of up to 20% in measurement accuracy, and further improvements can be expected with optimized designs. Applications for this test structure may include: monitoring the self-registration accuracy and precision of primary pattern generator systems and monitoring level-to-level overlay in advanced wafer fabrication.

[Contact: Michael W. Cresswell, (301) 975-2072]

Jones, M.A., Roberts, J.A., Ellenwood, C.H., Cresswell, M.W., and Allen, R.A., **Test Chip for the Evaluation of Surface-Diffusion Phenomena in Sputtered Aluminum Planarization Processes**, Proceedings of the IEEE 1991 International Conference on Microelectronic Test Structures, Kyoto, Japan, March 18-20, 1991, Vol. 4, No. 1, pp. 35-40 (1991).

A test chip has been designed and fabricated to enable the evaluation of surface diffusion phenomena in sputtered aluminum planarization processes. New and unique features provide for cross-sectioning bevel angle validation for SEM inspection, multiple design rules for planarization parameter optimization, and positive feature identification for step coverage evaluation. The results presented here demonstrate how the test chip is used to customize the deposition process variables for particular IC fabrication applications.

[Contact: Colleen H. Ellenwood, (301) 975-2236]

Khera, D., Cresswell, M.W., Linholm, L.W., Ramanathan, G., Buzzeo, J., and Nagarajan, A., **Knowledge Extraction Techniques for Expert System Assisted Wafer Screening**, Proceedings of the International Semiconductor Manufacturing Science Symposium, Burlingame, California, May 21-23, 1990, pp. 44-49 (1990).

This paper describes a procedure for using induction-based classification techniques for identifying relationships between work-in-process (WIP) test structure data and future IC yield at wafer test on a wafer-by-wafer or lot-by-lot basis. The relationships are extracted from databases of previously processed WIP wafer test structure measurements and final wafer yield. They are presented in the form of rules relating WIP data to final yield. It is further shown that these rules, when incorporated into expert systems, can advise the human operator responsible for screening wafers which are likely to produce sub-marginal yield if processed to completion. These rules also identify the WIP test structure parameters and values which have historically provided the highest and lowest final wafer yields.

[Contact: Dheeraj Khera, (301) 975-2240]

Kopanski, J.J., Carver, G.P., Lowney, J.R., Miles, D.S., and Novotny, D.B., **High Spatial Resolution Mapping of Semiconductor Resistivity**, Extended Abstract, Electrochemical Society Spring Meeting, Washington, D.C., May 5-10, 1991, Vol. 91-1, pp. 698-699 (1991).

A new approach to the resistivity mapping of semiconductors uses an array of lithographically defined contacts (at a density of 60,000 sites per cm^2) and an automated probe station for data acquisition. Resistivity growth striations in silicon as narrow as 45 μm in width and with $\pm 5\%$ variation from the background resistivity have been resolved. Solution of the Laplace equation for the measurement geometry and measurements on ion-implanted test structures are described. Anticipated

applications include resistivity mapping of liquid-encapsulated Czochralski GaAs, $\text{Hg}_{1-x}\text{Cd}_x\text{Te}$, and fine-scale resistivity variations in processed silicon.

[Contact: Joseph J. Kopanski, (301) 975-2089]

Schafft, H.A., **Measurement, Use, and Interpretation of TCR**, 1990 Workshop Final Report, 1990 International Wafer Level Reliability Workshop, Lake Tahoe, California, October 7-10, 1990, pp. 211-217 (1991).

A few comments are given about the measurement, use, and interpretation of the temperature coefficient of resistance (TCR). TCR is important when the determination of the temperature of a metallization line in an electromigration stress test is needed.

[Contact: Harry A. Schafft, (301) 975-2234]

Released for Publication

Allen, R.A., Cresswell, M.W., and Buck, L.M., **A New Test Structure for the Electrical Measurement of the Width of Short Features with Arbitrarily Wide Voltage Taps**.

Accurate determination of the linewidth of a narrow, conducting film for VLSI applications using electrical test structure metrology has required that the length of the line be many times its width to minimize geometric error due to finite width voltage taps. However, long lines obscure important local effects such as nonuniformities in the film. Shorter lines highlight such effects. This paper describes a method of measuring the width of a short line having taps of arbitrary width. The effect of the taps is measured and used in the extraction of the linewidth allowing the confident determination of local linewidth variations.

[Contact: Richard A. Allen, (301) 975-5026]

Khera, D., Cresswell, M.W., Linholm, L.W., Ramanathan, G., Nagarajan, R., and Buzzeo, J.M., **Knowledge Extraction Techniques for Wafer Screening Using Expert Systems**.

This paper describes a procedure for using induction-based classification techniques for identifying relationships between work-in-process (WIP) test structure data and future IC yield at wafer test on a wafer-by-wafer or lot-by-lot basis. The relationships are extracted from databases of previously processed WIP wafer test structure measurements and final wafer yield. They are presented in the form of rules relating WIP data to final yield. It is further shown that these rules,

when incorporated into expert systems, can advise the human operator responsible for screening wafers which of the wafers are likely to produce sub-marginal yield if processed to completion. These rules also identify the WIP test structure parameters and values which have historically provided the highest and lowest final wafer yields.

[Contact: Raj Khera, (301) 975-2240]

Suehle, J.S., and Schafft, H.A., **Techniques and Characterization of Pulsed Electromigration at the Wafer Level**, to be published in the Proceedings of Relectronic '91, Budapest, Hungary, August 26-30, 1991.

Special testing techniques were developed to circumvent problems associated with high temperature wafer-level probing and pulsed stressing of Al-Si metallizations. Recent results, using these techniques, identify new measurement interferences for highly accelerated electromigration stress tests. Measurements of the median time to failure, t_{50} , for dc and for pulsed current stress as a function of pulse repetition frequency reveal that highly accelerated stress tests may overestimate metallization reliability.

[Contact: John S. Suehle, (301) 975-2247]

Microfabrication Technology

Recently Published

Dagata, J.A., Schneir, J., Harary, H.H., Bennett, J., and Tseng, W.F., **Pattern Generation on Semiconductor Surfaces by a Scanning Tunneling Microscope Operating in Air**, *Journal of Vacuum Science Technology B*, Vol. 9, No. 2, pp. 1384-1388 (Mar./Apr. 1991). (Proceedings of the Scanning Tunneling Microscopy '90/Nanometer Scale Science and Technology Symposium I, Baltimore, Maryland, July 23-27, 1990.)

Recent results employing scanning tunneling microscope-based techniques for the generation of nanometer-scale patterns on passivated semiconductor surfaces are presented. Preparation and characterization of hydrogen-passivated silicon and sulfur-passivated gallium arsenide surfaces are described, and the determination of the chemical and morphological properties of the patterned regions by scanning electron microscopy and time-of-flight secondary ion mass spectrometry are discussed. Our recent demonstration that ultra-shallow, oxide features written by an STM can serve as an effective mask for selective-area GaAs heteroepitaxy on

silicon is used to illustrate key requirements necessary for the realization of a unique, STM-based nanotechnology.

[Contact: Wen F. Tseng, (301) 975-5291]

Dagata, J.A., Tseng, W., Bennett, J., Evans, C.J., Schneir, J., and Harary, H.H., **Selective-Area Epitaxial Growth of Gallium Arsenide on Silicon Substrates Patterned Using a Scanning Tunneling Microscope Operating in Air**, *Applied Physics Letters*, Vol. 57, No. 23, pp. 2437-2439 (3 December 1990).

Selective-area epitaxial growth of gallium arsenide on n-Si(100) substrates is reported, where the oxide (SiO_2) mask consists of 1 to 2 monolayer-thick features patterned onto a silicon substrate using a scanning tunneling microscope (STM) operating in air. The technique for generating the STM patterns on hydrogen-passivated silicon was reported recently. The GaAs epilayer was grown by migration-enhanced epitaxy at 580 °C, and its morphology was investigated by scanning electron microscopy. The chemical selectivity of the STM-patterned regions was verified by imaging time-of-flight secondary-ion mass spectrometry. The implications of these results for the development of a unique, STM-based nanostructure fabrication technology are discussed.

[Contact: Wen F. Tseng, (301) 975-5291]

Myers, D.R., Dawson, L.R., Klem, J.F., Brennan, T.M., Hammons, B.E., Simons, D.S., Comas, J., and Pellegrino, J.G., **Unintentional Indium Incorporation in GaAs Grown by Molecular Beam Epitaxy**, *Applied Physics Letters*, Vol. 57, No. 22, pp. 2321-2323 (26 November 1990).

We have characterized unintentional indium incorporation into GaAs grown by molecular-beam epitaxy in a variety of commercial molecular-beam epitaxy systems. We find that the unintentional indium-doping level in the epitaxial GaAs during growth is more a function of mounting technique and prior machine history than of the manufacturer's design. The indium doping detected in the epitaxial GaAs for substrates that only partially obscure an indium-bearing mount is equal to levels reported to result in minimum defect densities and narrowest photoluminescence linewidths in In-doped GaAs.

[Contact: Joseph G. Pellegrino, (301) 975-2123]

Zavada, J.M., Wilson, R.G., and Comas, J., **Redistribution of H and Be in GaAs/AlAs Multilayer Structures with Post-Implantation Annealing**, *Journal*

of Applied Physics, Vol. 65, No. 5, pp. 1968-1971 (1 March 1989).

The redistribution of implanted atoms within GaAs/AlAs multilayer structures due to post-implantation furnace annealing is reported. The structures were grown using molecular-beam epitaxy on GaAs substrates and implanted with either hydrogen or beryllium ions. After furnace annealing at temperatures up to 700 °C, these samples were examined using secondary ion mass spectrometry. The measurements show that the hydrogen and the beryllium atoms redistribute with post-implantation annealing and that both species accumulate at the buffer layer-substrate interface. The concentration of atoms at this interface can exceed $1 \times 10^{19} \text{ cm}^{-3}$ and may be related to the crystal imperfections created during the initial stages of epitaxy. The significant redistribution of implanted ions may also alter the optoelectronics properties of multilayer semiconductor structures processed in this manner.
[Contact: James Comas, (301) 975-2061]

Released for Publication

Miller, W.R., Jr., Boettinger, W.J., Tseng, W.F., Pellegrino, J.G., and Comas, J., **Controlled Interface Roughness in GaAs/AlAs Superlattices**, to be published in the Proceedings of the Materials Research Society 1991 Spring Meeting, Anaheim, California, April 29-May 2, 1991.

We report the results of our study of controlled interface roughness in low-order GaAs/AlAs superlattices. Samples were prepared using either the interrupted growth or the migration-enhanced epitaxy (MEE) technique. The samples were prepared with m atomic planes of GaAs and m atomic planes of AlAs ($m \times m$) per modulation wavelength and repeated p times. For this study, $m = 1$ or 3 . The samples were studied using X-ray diffraction. The interrupted growth samples both showed a split in one diffraction line, indicating layers were not of integral order, while the MEE samples showed no splitting, indicating integral order layers.
[Contact: James Comas, (301) 975-2061]

Pellegrino, J.G., Qadri, S., Tseng, W.F., and Comas, J., **Periodicities Associated with Low-Order AlAs/GaAs Superlattices**, to be published in the Proceedings of the International Conference of Metallurgical Coatings and Thin Films '91, San Diego, California, April 1991.

The use of molecular beam epitaxy to produce

heterostructures has made it possible to examine superlattices with monolayer and submonolayer period spacings. In this work we examine the physical properties for the superlattice system $(\text{GaAs})_{n_1}(\text{AlAs})_{n_2}/\text{GaAs}(001)$ for low values of n_1 and n_2 , i.e., $n_1 = n_2 = 3, 6, 12$. Normal, interrupted growth, and migration-enhanced epitaxy growth techniques were used to grow superlattice structures, and X-ray diffraction was used to analyze the major and satellite peak positions. An analysis of the major diffraction peaks and their associated satellites exhibited superlattice periodicity in good agreement with theory. Diffraction peaks were also observed in regions adjacent to the primary diffraction peaks which did not occur in the expected satellite positions. An analysis of these peaks relative to the primary peaks indicate periodicities which are greater than the intended period. One possible cause for these periodicities is variations in growth conditions which occur while the superlattice is being grown. An understanding of low-order superlattices is important for structures which are dependent upon interface sharpness.
[Contact: Joseph G. Pellegrino, (301) 975-2123]

Pellegrino, J.G., Qadri, S., Tseng, W.F., Miller, W.R., and Comas, J., **Periodicities in the X-ray Diffraction of Low Order AlAs/GaAs Superlattices**, to be published in the Proceedings of the Material Research Society 1991 Spring Meeting, Anaheim, California, April 29-May 2, 1991.

In this work, we examine the physical properties for the superlattice system $(\text{GaAs})_{n_1}(\text{AlAs})_{n_2}/\text{GaAs}(100)$ for low values of n_1 and n_2 , i.e., $n_1 = n_2 = 3, 6, 12$. Normal, interrupted growth, and migration-enhanced epitaxy growth techniques were used to grow the superlattice structures in a molecular beam epitaxy system. X-ray diffraction spectra were obtained, and the major and satellite peak positions were analyzed to obtain the superlattice periodicity. An analysis of the major diffraction peaks and their associated satellites produced superlattice periodicity in good agreement with theory. Diffraction peaks were also observed in regions adjacent to the primary diffraction peaks which did not occur in the expected satellite positions. An analysis of these peaks relative to the primary peak indicate periodicities corresponding to layer thickness greater than the intended period. One possible cause for these periodicities is growth conditions that exist during the growth of the superlattice which result in the deposition of fractional monolayers. In this study, we present results which suggest that an arsenic-deficient growth condition may be a contributing factor in the deposition

of fractional monolayers.

[Contact: Joseph G. Pellegrino, (301) 975-2123]

Tseng, W.F., Pellegrino, J.G., Kim, J.S., Thurber, W.R., Comas, J., Papanicolou, N., and Prokes, S., **Reduction of DX Centers in Superlattice Alloylike Material (SLAM) HEMTs.**

The substitution of selectively Si-doped short-period (4 by 2 and 2 by 1 monolayer(s)) GaAs/AlAs superlattice alloylike material (SLAM) for Si-doped AlGaAs layers in conventional high-electron-mobility transistor (HEMT) structures has been demonstrated. Such a short period SLAM HEMT still preserves its field-effect transistor characteristics as compared with the conventional HEMT. The shifts of threshold voltages and amounts of DX centers were found to depend on the layer thickness of the superlattices and the positions of Si-dopants within the GaAs layers.

[Contact: Wen F. Tseng, (301) 975-5291]

Plasma Processing

Recently Published

Roberts, J.R., Olthoff, J.K., Van Brunt, R.J., and Whetstone, J.R., **Measurements on the NIST GEC Reference Cell**, Proceedings of SPIE (The International Society for Optical Engineering, P.O. Box 10, Bellingham, Washington 98227-0010), *Advanced Techniques for Integrated Circuit Processing*, Vol. 1392, pp. 428-436 (1990).

Measurements performed on the NIST GEC Reference Cell are described. The Reference Cell concept grew out of a workshop held at the 1988 Gaseous Electronics Conference (GEC) (October 18-22, 1988, Minneapolis, Minnesota). The design was refined by the GEC community, reviewed at a workshop hosted by SEMATECH (March 9, 1989), and the final design was engineered at Sandia National Laboratory. The purpose of the discharge cell is to provide an affordable experimental platform for researchers that is physically identical from laboratory to laboratory, so that reference data can be generated and various experimental techniques and models can be cross correlated. Four laboratories (Sandia, AT&T Bell Labs, Wright-Patterson Air Force Base, and NIST) agreed to conduct identical initial measurements on four cells manufactured at the same time. This would ensure the greatest possible uniformity and allow direct comparison of results. The experimental conditions for the present measurements are those specified for intercomparison and include 1-in.

interelectrode spacing, grounded lower electrode, capacitively coupled RF power, cooled electrodes (20 °C), electrode ground shields and 99.999% argon. The specific measurements to be made were: 1) the waveforms of the fundamental through the fifth harmonic of the rf voltage and current, including their magnitude and phase; 2) the gas flow rate and pressure; and 3) the dc self-bias voltage.

[Contact: James K. Olthoff, (301) 975-2431]

Power Devices

Recently Published

Berning, D.W., **An Automated Reverse-Bias Second-Breakdown Transistor Tester**, Proceedings of the Applied Power Electronics Conference and Exposition, Dallas, Texas, March 10-15, 1991, pp. 339-346 (1991). [Also published in the *Journal of Research of the National Institute of Standards and Technology*, Vol. 96, No. 3, pp. 291-304 (May-June 1991).]

An automated instrument is described for nondestructively generating curves for the reverse-bias, safe-operating area of transistors. A new technique for detecting second breakdown that makes automation possible is highlighted. Methods to reduce stress to the device under test are discussed, as are several other innovations that enhance automation. Measurements using the tester are described, and limitations on nondestructive testability are discussed.

[Contact: David W. Berning, (301) 975-2069]

Photodetectors

Recently Published

Kohler, R., Geist, J., and Bonhoure, J., **Generalized Photodiode Self-Calibration Formula**, *Applied Optics*, Vol. 30, No. 7, pp. 884-886 (1 March 1991).

We have derived the photodiode self-calibration formula for calculating the internal quantum efficiency of silicon photodiodes from the results of up to three independent self-calibration experiments, and from the results of the oxide-bias and reverse-bias experiments in conjunction with a calculation of the effect of Auger recombination. We show that the formula published elsewhere for these three effects is not correct.

[Contact: Jon Geist, (301) 975-2066]

Released for Publication

Geist, J., Robinson, A.M., and James, C.R., **Numerical Modeling of Silicon Photodiodes for High-Accuracy Applications. Part III: Interpolating and Extrapolating Internal Quantum-Efficiency Calibrations**, to be published in the Journal of Research of the National Institute of Standards and Technology.

The semiconductor device modeling program PC-1D and the programs that support its use in high-accuracy modeling of photodiodes, all of which were described in Part I, are used to simulate the interpolation of high-accuracy internal quantum-efficiency calibrations near 450 nm and 850 nm to the spectral region between these wavelengths. Convenient interpolation formulae that depend only upon wavelength are derived, as are uncertainty spectra for a number of sources of error. The formulae are normalized to experimental internal quantum-efficiency calibrations in the 440- to 470-nm spectral region and at 860 nm, and used to interpolate the calibrations to intermediate wavelengths. The results of the interpolations are compared with experimental calibration data that are available at a few wavelengths between 440 and 860 nm. The disagreement between the interpolated and measured internal quantum-efficiency data is never worse than 0.0003. [Contact: Jon Geist, (301) 975-2066]

Reliability

Recently Published

Kopanski, J.J., Blackburn, D.L., Harman, G.G., and Berning, D.W., **Assessment of Reliability Concerns for Wide-Temperature Operation of Semiconductor Devices and Circuits**, Proceedings of the First International High Temperature Electronics Conference, Albuquerque, New Mexico, June 16-20, 1991, pp. 137-142 (1991).

Factors that may affect the long-term (30 yrs $\approx 10^6$ h) reliability of electronic systems that can withstand temperature extremes (-150 to +300 °C) are discussed. There is ample evidence that a straightforward application of the Arrhenius equation, with activation energies determined from high-temperature accelerated stress testing, is not strictly valid for predicting real device lifetime. The relevance and validity of this traditional reliability assurance methodology, especially near the high-temperature operating limit, is critiqued. Some of the barriers to long-term reliable operation of devices and circuits subject to extreme temperatures are identified in the broad areas of: (1) semiconductor

materials, (2) components and circuit design, and (3) packaging and assembly. Finally, alternative approaches to reliability assurance, not dependent on elevated temperature testing, which may be applicable to high-temperature electronics, are discussed. [Contact: Joseph J. Kopanski, (301) 975-2089]

Schafft, H.A., Baglee, D.A., and Kennedy, P.E., **Building-In Reliability: Making It Work**, Proceedings of the 1991 International Reliability Physics Symposium, Las Vegas, Nevada, April 9-11, 1991, pp. 1-7 (1991). [Also published in RAC Quarterly, Vol. 1, No. 2, pp. 2-9 (Spring 1991).]

Aggressive reliability and market-entry demands will require the use of a building-in approach to reliability. To adopt this approach and make it work require that very significant breaks be made from the traditional ways of improving and appraising reliability. The nature of these breaks are discussed in the context of describing the basic elements of the approach of building-in reliability and the obstacles that hinder its adoption. To help visualize how the approach can be implemented, initial steps to make the transition and some specific examples of its use are described.

[Contact: Harry A. Schafft, (301) 975-2234]

SIGNAL ACQUISITION, PROCESSING, & TRANSMISSION

DC & Low Frequency Metrology

Recently Published

Cage, M.E., Yu, D., Jeckelmann, B.M., Steiner, R.L., and Duncan, R.V., **Investigating the Use of Multimeters to Measure Quantized Hall Resistance Standards**, IEEE Transactions on Instrumentation and Measurement (Special Issue of selected papers, CPEM '90), Vol. 40, No. 2, pp. 262-266 (April 1991). [Also published in the Digest of the 1990 Conference on Precision Electromagnetic Measurements, Ottawa, Canada, June 11-14, 1990, pp. 332-333 (1990).]

A new generation of digital multimeters was used to directly compare the ratios of the resistances of wire-wound reference resistors and quantized Hall resistances. The accuracies are better than 0.1 parts per million for ratios as large as 4:1 if the multimeters are calibrated with a Josephson array.

[Contact: Marvin E. Cage, (301) 975-4249]

Filipski, P.S., So, E., Moore, W.J.M., Knight,

R.B.D., Martin, P., Oldham, N.M., and Waltrip, B.C., **An International Comparison of Low Audio Frequency Power Meter Calibrations Conducted in 1989**, IEEE Transactions on Instrumentation and Measurement (Special Issue of selected papers, CPEM '90), Vol. 40, No. 2, pp. 399-402 (April 1991). [Also published in the Digest of the 1990 Conference on Precision Electromagnetic Measurements, Ottawa, Canada, June 11-14, 1990, pp. 158-159 (1990).]

The results of an intercomparison of low-audio-frequency power meter calibrations conducted in 1989 between the National Research Council (NRC), Canada, the National Physical Laboratory (NPL), United Kingdom, and the National Institute of Standards and Technology (NIST), USA, are described. A time-division watt-converter, developed at NRC, was used as the transfer standard. The measurements were made at 120 V, 5 A, power factors of 1, 0 lead, and 0 lag and at frequencies up to 5 kHz. Agreement between the NPL and NRC laboratories was better than 63 parts per million in the 60- to 1600-Hz range, 74 parts per million between NIST and NRC in the 50- to 4800-Hz range. [Contact: Nile M. Oldham, (301) 975-2408]

Huang, D.X., Kinard, J.R., and Rebuldele, G., **RF-DC Differences of Thermal Voltage Converters Arising from Input Connectors**, IEEE Transactions on Instrumentation and Measurement (Special Issue of selected papers, CPEM '90), Vol. 40, No. 2, pp. 360-365 (April 1991). [Also to be published in the Digest of the 1990 Conference on Precision Electromagnetic Measurements, Ottawa, Canada, June 11-14, 1990.]

The rf-dc differences of thermal voltage converters (TVCs) caused by skin effect and transmission-line effects of different length input structures have been studied. Some discrepancies do exist between simple mathematical models and measured results for commonly used input connectors. This paper reports a study of these discrepancies and some worst-case results of changes in rf-dc difference due to connection and disconnection of TVCs.

[Contact: Joseph R. Kinard, (301) 975-4250]

Kinard, J.R., Lipe, T.E., and Childers, C.B., **AC-DC Difference Relationships for Current Shunt and Thermal Converter Combinations**, IEEE Transactions on Instrumentation and Measurement (Special Issue of selected papers, CPEM '90), Vol. 40, No. 2, pp. 352-355 (April 1991). [Also published in the Digest of the 1990 Conference on Precision Electromagnetic Measurements, Ottawa, Canada, June 11-14, 1990, pp.

136-137 (1990).]

This paper describes the relationship between the overall ac-dc difference of a thermal converter and current shunt combination and the characteristics of the separate thermal converter and current shunt. As a consequence of the analysis, an expression predicting the ac-dc difference of a thermal converter/shunt combination when thermoelements are interchanged is presented, and data illustrating the agreement between values of ac-dc difference and values predicted by the analysis are given. [Contact: Joseph R. Kinard, (301) 975-4250]

Oldham, N.M., and Henderson, R.M., **New Low-Voltage Standards in the DC to 1 MHz Frequency Range**, IEEE Transactions on Instrumentation and Measurement (Special Issue of selected papers, CPEM '90), Vol. 40, No. 2, pp. 368-372 (April 1991). [Also published in the Digest of the 1990 Conference on Precision Electromagnetic Measurements, Ottawa, Canada, June 11-14, 1990, pp. 66-67 (1990).]

Several new techniques for measuring the rms value of 1- to 200-mV signals have been developed and compared to existing techniques using thermal transfer standards. Differences between the various measurement methods at 100 mV are typically within ± 100 parts per million from dc to 1 MHz.

[Contact: Nile M. Oldham, (301) 975-2408]

Oldham, N.M., and Nelson, T.L., **Influence of Nonsinusoidal Waveforms on Voltmeters, Ammeters, and Phasemeters**, Proceedings of the IEEE Winter Power Meeting, New York, New York, February 3-7, 1991, pp. 7-12 (1991).

The operating principles of various voltmeters, ammeters, and phasemeters are described. The results of tests of these instruments at different levels of distortion indicate that phasemeters are subject to large, often unpredictable errors while most voltmeters and ammeters respond to the rms value, independent of waveshape.

[Contact: Nile M. Oldham, (301) 975-2408]

Steiner, R.L., and Astalos, R.J., **Improvements for Automating Voltage Calibrations Using a 10-V Josephson Array**, IEEE Transactions on Instrumentation and Measurement (Special Issue of selected papers, CPEM '90), Vol. 40, No. 2, pp. 321-325 (April 1991). [Also published in the Digest of the 1990 Conference on Precision Electromagnetic Measurements, Ottawa, Canada, June 11-14, 1990, pp.

102-103 (1990).]

A voltage standard system based on a 10-V Josephson array has been completely automated with three novel developments. First, a unique way of connecting zener voltage standards, a digital voltmeter, and the array to a commercial standard cell scanner has provided necessary switching flexibility. Second, using a programmable millimeter-wave attenuator has greatly simplified the selection of voltage steps. Third and last, programmed error checking, which verifies array steps by comparing measurement scatter to previously characterized system noise levels, has proven more reliable than visual observation. The operation of this new system is simplified enough for an inexperienced user while the calibration uncertainty (1σ) is still a few parts in 10^8 . [Contact: Richard L. Steiner, (301) 975-4226]

Waltrip, B.C., and Oldham, N.M., **Performance Evaluation of a New Audio-Frequency Power Bridge**, IEEE Transactions on Instrumentation and Measurement (Special Issue of selected papers, CPEM '90), Vol. 40, No. 2, pp. 380-383 (April 1991). [Also published in the Digest of the 1990 Conference on Precision Electromagnetic Measurements, Ottawa, Canada, June 11-14, 1990, pp. 142-143 (1990).]

Several techniques for measuring active and reactive power in the 50-Hz to 20-kHz frequency range are described. The approaches include: (1) the development of a high-precision sampling wattmeter using a resistive attenuator, a shunt, and two commercially available sampling voltmeters configured as a dual-channel equivalent-time sampler; (2) the development of another high-precision sampling wattmeter using the same shunt and attenuator, a high-impedance, wideband differential amplifier, and a commercially available, dual-channel, direct-sampling waveform analyzer; (3) for zero power factor measurements, the use of a digital generator to produce precise phase shifts from $+\pi/2$ to $-\pi/2$; and (4) the use of simultaneous thermal voltage and current measurements for unity power factor measurements. These approaches were developed to evaluate a new high-accuracy, audio-frequency power bridge that is based on ac voltage and impedance measurements. [Contact: Bryan C. Waltrip, (301) 975-2438]

Released for Publication

Elmqvist, R.E., and Dziuba, R.F., **Isolated Ramping Current Sources for a Cryogenic Current Comparator Bridge**.

The design and performance of a pair of highly isolated ramping and reversing direct current sources for use with a cryogenic current comparator resistance bridge and dc SQUID detector are described. The current sources are floating and isolated from each other, and are internally programmed to reverse the output current while maintaining the SQUID feedback control system in lock. Sources have been constructed with full-scale current ranges from 0.65 mA to 100 mA and have been used in the comparisons of precision standard resistors at the 0.01 parts-per-million level.

[Contact: Randolph E. Elmqvist, (301) 975-6591]

Waveform Metrology

Recently Published

Oldham, N.M., and Nelson, T.L., **Influence of Nonsinusoidal Waveforms on Voltmeters, Ammeters, and Phasemeters**, Proceedings of the IEEE Winter Power Meeting, New York, New York, February 3-7, 1991, pp. 7-12 (1991).

The operating principles of various voltmeters, ammeters, and phasemeters are described. The results of tests of these instruments at different levels of distortion indicate that phasemeters are subject to large, often unpredictable errors, while most voltmeters and ammeters respond to the rms value, independent of waveshape.

[Contact: Nile M. Oldham, (301) 975-2408]

Waltrip, B.C., and Oldham, N.M., **Performance Evaluation of a New Audio-Frequency Power Bridge**, IEEE Transactions on Instrumentation and Measurement (Special Issue of selected papers, CPEM '90), Vol. 40, No. 2, pp. 380-383 (April 1991). [Also published in the Digest of the 1990 Conference on Precision Electromagnetic Measurements, Ottawa, Canada, June 11-14, 1990, pp. 142-143 (1990).]

Several techniques for measuring active and reactive power in the 50-Hz to 20-kHz frequency range are described. The approaches include: (1) the development of a high-precision sampling wattmeter using a resistive attenuator, a shunt, and two commercially available sampling voltmeters configured as a dual-channel equivalent-time sampler; (2) the development of another high-precision sampling wattmeter using the same shunt and attenuator, a high-impedance, wideband differential amplifier, and a commercially available, dual-channel, direct-sampling waveform analyzer; (3) for zero power factor

measurements, the use of a digital generator to produce precise phase shifts from $+\pi/2$ to $-\pi/2$; and (4) the use of simultaneous thermal voltage and current measurements for unity power factor measurements. These approaches were developed to evaluate a new high-accuracy, audio-frequency power bridge that is based on ac voltage and impedance measurements.

[Contact: Bryan C. Waltrip, (301) 975-2438]

Released for Publication

Oldham, N.M., and Hetrick, P.S., **High Frequency, High Speed Phase Angle Measurements and Standards**, to be published in the Proceedings of the 1991 National Conference of Standards Laboratories Workshop and Symposium, Albuquerque, New Mexico, August 19-22, 1991.

Counter-timers capable of measuring the delay between two signals at frequencies up to 20 MHz have been evaluated as phase angle meters with applications in heterodyne interferometry. A scheme for calibrating these instruments, both statically and dynamically (with the phase angle changing as fast $10^\circ/\mu\text{s}$), is described.

[Contact: Nile M. Oldham, (301) 975-2408]

Cryoelectronic Metrology

Released for Publication

Barmak, K., Coffey, K.R., Foner, S., and Rudman, D.A., **Effect of Microstructure on Phase Formation in the Reaction of Nb/Al Multilayer Thin Films**, to be published in the Proceedings of the Materials Research Society Spring Meeting, Anaheim, California, April 29-May 3, 1991.

We investigated the phase formation sequence in the reaction of multilayer thin films of Nb/Al with overall compositions of 25 and 33 atomic percent Al. We report novel phenomena which distinguish thin-film reactions unequivocally from those in bulk systems. For sufficiently thin layers, composition and stability of product phases are found to deviate significantly from that predicted from the equilibrium phase diagram. We demonstrate that in the Nb/Al system, the length scales below which such deviations occur is about 150 nm. We believe that these phenomena occur due to the importance of grain boundary diffusion and, hence, microstructure in these thin films.

[Contact: David A. Rudman, (303) 497-5081]

Coffey, K.R., Barmak, K., Rudman, D.A., and Foner, S.,

First Phase Formation Kinetics in the Reaction of Nb/Al, to be published in the Proceedings of the Materials Research Society Spring Meeting, Anaheim, California, April 29-May 3, 1991.

Phase formation kinetics in Nb/Al multilayered thin films were investigated using scanning calorimetry, X-ray diffraction, and cross-sectional transmission electron microscopy. The first phase to form upon annealing the Nb/Al layered structure is the NbAl_3 intermetallic. Its formation is clearly identified by the calorimetry to be a two-stage process, which has been modeled as the nucleation and three-dimensional growth to coalescence of the product phase in the plane of the initial interface, followed by the thickening of the product layer by one-dimensional growth perpendicular to the interface plane. For the initial reaction stage, the reaction front velocity is higher than can be supported by diffusional transport within the lattices adjacent to the moving interface. Thus, diffusion along nonequilibrium interfaces is the growth mechanism. The large volume fraction consumed during the initial reaction stage indicates a lower nucleation site density than expected at the Nb/Al equilibrium interface, suggesting that the interface transport is reducing the driving force for nucleation.

[Contact: David A. Rudman, (303) 497-5081]

Coffey, K.R., Barmak, K., Rudman, D.A., and Foner, S., **Thin Film Reaction Kinetics of Niobium/Aluminum Multilayers**.

Phase formation kinetics in Nb/Al multilayered thin films having overall compositions of 25, 33, 50, and 75 atomic percent Al have been investigated using scanning calorimetry, X-ray diffraction, and cross-sectional transmission electron microscopy. The first phase to form upon annealing the Nb/Al layered structure of all samples is the NbAl_3 intermetallic. The NbAl_3 formation is clearly identified by the calorimetry to be a two-stage process. The first stage is the formation of a planar layer by nucleation and growth to coalescence, while the second stage is the thickening of the planar layer. The large heat effect for the first reaction stage is consistent with heterogeneous nucleation at well-isolated sites in the Nb/Al interface. This is surprising in light of the large thermodynamic driving force expected for nucleation, and suggests that the local nonequilibrium nature of the Nb/Al interface greatly reduces the driving force for nucleation. The next phase observed to grow in samples of 25 and 33 atomic percent Al is the A15 superconducting phase, Nb_3Al . The Nb_3Al growth completes a first reaction stage similar to the NbAl_3 , but the subsequent thickening reaction stage is

not observed without simultaneous Ab_2Al growth. The high interface velocities derived from the calorimetry results for formation of both NbAl_3 and the $\text{Al}_5\text{Nb}_3\text{Al}$ indicate that the atomic transport must be by grain boundary diffusion.

[Contact: David A. Rudman, (303) 497-5081]

Condron, M.R., Gutt, G.M., Mulfelder, B., Lockhart, J.M., Turneure, J.P., Huber, M.E., Cromar, M.W., and Houseman, E.K., **Noise Measurements on dc SQUIDs with Varied Designs**, to be published in the Proceedings of SQUID '91, Heidelberg, Germany, June 18-21, 1991.

We have fabricated and tested two types of SQUIDs. The first, a low inductance stripline device, was characterized using a commercial dc SQUID as a following amplifier. The second type was well coupled to a $0.16\text{-}\mu\text{H}$ input coil and was characterized and flux-locked using an ultra-low noise room temperature preamplifier. We present device characterization and noise data for both types of devices.

[Contact: Martin E. Huber, (303) 497-5423]

Lichtenwalner, D.J., Anderson, A.C., and Rudman, D.A., **Modeling of the Reactive Sputtering Process, and Comparison with Experimental Results**.

In this report, we present a model to describe the reactive sputtering process. This model treats the reactive sputtering process as a flux balance between the reacting species of interest. Sputtering yields are used to describe the sputtering rates, and sticking coefficients are used to describe reaction rates. For the Ar-ion-beam sputtering of Nb target with N_2 added, the model accurately fits the measured N_2 pressure and deposition rate as a function of the N_2 flow. The fit to the measured data allows values of fundamental parameters such as the sticking coefficient of nitrogen and sputtering yields to be extracted. The values of all extracted model parameters are physically consistent, verifying the applicability of the model. Modeled fits to the measured data reveal that the thermal N_2 molecules are very reactive, controlling the target reaction process even with N_2^+ ions present in the ion beam. Values of the sputtering yields and sticking coefficients extracted from model fits to the measured data enable predictions to be made of (as yet) unmeasured quantities, such as the sputtered flux ratio of N to Nb from the reacted target. An interesting prediction of the model is that the sputtered flux of N can actually exceed the sputtered flux of Nb once the target surface has reacted sufficiently. This represents a significant difference

between reactive sputtering and the sputtering of a compound target. These sputtered reactive species would control the reaction process for material systems in which the molecule is not very reactive but the atom is reactive.

[Contact: David A. Rudman, (303) 497-5081]

Antenna Metrology

Released for Publication

Francis, M.H., and Wittmann, R.C., **Swept Frequency Gain Measurements From 33-50 GHz at the National Institute of Standards and Technology**, to be published in the Proceedings of the Antenna Measurement Techniques Association 13th Annual Meeting and Symposium, Boulder, Colorado, October 7-11, 1991.

As part of an effort to provide improved measurement services at frequencies above 30 GHz, scientists at the National Institute of Standards and Technology have completed development of a swept frequency gain measurement service for the 33- to 50-GHz band. This service gives gain values with an accuracy of ± 0.3 dB. In this paper, we discuss an example measurement and the associated errors.

[Contact: Michael H. Francis, (303) 497-5873]

Noise Metrology

Recently Published

Wait, D.F., **Comments Concerning On-Wafer Noise Parameter Measurements**, Conference Digest, 36th ARFTG Conference, Monterey, California, November 29-30, 1990, pp. 5-15 (1991).

The National Institute of Standards and Technology (NIST) has a goal of offering an on-wafer noise parameter special test service in 1992. This paper describes two phases of this project. This includes a discussion of the equipment and techniques recently used at NIST to measure the noise parameters of low-noise 8- to 12-GHz amplifiers, and some simple measurements to demonstrate deembedding a wafer probe for a measurement of amplifier noise on-wafer.

[Contact: David F. Wait, (303) 497-3610]

Wait, D.F., Counas, G.J., Kessel, W., and Buchholz, F.I., **PTB-NIST Bilateral Comparison of Microwave Noise Power in Coaxial Transmission Line**, IEEE Transactions on Instrumentation and Measurement (Special Issue of selected papers, CPEM

'90), Vol. 40, No. 2, pp. 449-454 (April 1991). [Also published in the Digest of the 1990 Conference on Precision Electromagnetic Measurements, Ottawa, Canada, June 11-14, 1990, pp. 34-35 (1990).]

The Physikalisch-Technische Bundesanstalt (PTB) and the National Institute of Standards and Technology (NIST) have compared microwave noise power in coaxial transmission lines. This intercomparison is of particular metrological interest as both laboratories have independently developed coaxial primary thermal noise standards using different technologies: a hot standard at PTB and cold standards at NIST.

Different types of comparison radiometers are operating at each laboratory: a total power radiometer at NIST and an RF-switched radiometer with IF-attenuator at PTB. Each laboratory measured two solid-state noise sources at 2.0, 4.0, and 8.0 GHz relative to their primary thermal noise standards. The agreement between laboratories is better than 0.05 dB.

[Contact: David F. Wait, (303) 497-3610]

Wait, D.F., and Engen, G.F., **Application of Radiometry to the Accurate Measurement of Amplifier Noise**, IEEE Transactions on Instrumentation and Measurement, Vol. 40, No. 2, pp. 433-437 (April 1991).

In response to the requirements of the microwave community which it serves, a calibration service for amplifier noise is under development at the National Institute of Standards and Technology (NIST). This paper includes a review and makes certain extensions to the associated theory from the scattering matrix context. Following this, the application of the (highly developed) NIST radiometers to the measurement problem is outlined, and a preliminary assessment of the probable accuracy is given.

[Contact: David F. Wait, (303) 497-3610]

Microwave & Millimeter-Wave Metrology

Recently Published

Marks, R.B., **A Multi-Line Calibration for MMIC Measurement**, Conference Digest, 36th ARFTG Conference, Monterey, California, November 29-30, 1990, pp. 47-55 (1991).

A modification of the through-reflect-line (TRL) calibration method provides enhanced network analyzer calibration for purposes of MMIC measurement. The method utilizes multiple, redundant transmission line

standards and relies on a statistical procedure to reduce the effects of random contact error. The covariance matrices necessary for the application of the procedure are developed as a result of a linearized error analysis of the basic TRL method. Simulated and measured calibrations demonstrate that the method is fast and accurate and increases the bandwidth of TRL calibrations.

[Contact: Roger B. Marks, (303) 497-3037]

Marks, R.B., and Williams, D.F., **Characteristic Impedance Determination Using Propagation Constant Measurement** [original title: Determination of Characteristic Impedance from Measurement of Propagation Constant], IEEE Microwave and Guided Wave Letters, Vol. 1, No. 6, pp. 141-143 (June 1991).

A method is demonstrated whereby the characteristic impedance of transmission lines may be easily determined from a measurement of the propagation constant. The method is based on a rigorous analysis using realistic approximations to account for the effects of imperfect conductors. Numerical studies indicate that high accuracy is possible, and experiments using coplanar waveguide demonstrate the advantage of the method in the interpretation of S-parameters.

[Contact: Roger B. Marks, (303) 497-3037]

Phillips, K.A., and Williams, D.F., **MMIC Package Characterization with Active Loads**, Conference Digest, 36th ARFTG Conference, Monterey, California, November 29-30, 1990, pp. 64-72 (1991).

A technique for characterizing microwave packages based on active PIN diode standards is discussed. The technique allows packages to be accurately characterized from external reflection coefficient measurements when a single bias-dependent active standard is embedded within it. The frequency characteristics, stability, and linearity of active PIN diode standards are investigated.

[Contact: Kurt A. Phillips, (303) 497-5383]

Vanzura, E.J., and Rogers, J.E., **Resonant Circuit Model Evaluation Using Reflected S-Parameter Data** [original title: Evaluation of a Resonant Circuit Model Using Reflected S-Parameter Data], IEEE Instrumentation and Measurement Technology Conference, Atlanta, Georgia, May 14-16, 1991, pp. 150-155 (1991).

A nonlinear regression procedure is used to fit S-parameter resonance data to a full-circuit model that

includes coupling factors and self-impedances. Such a model should provide an adequate mathematical representation of cavity resonator data. Our analysis shows that this model fits the data better than the simpler Q-circle model that can be derived from it, but that a systematic pattern in the residuals persists. This pattern indicates a discrepancy between the full-circuit model and the observed data. By looking at parameter estimates calculated from subsets of the original data, we demonstrate that the cause of this discrepancy could also be introducing significant errors in the model's estimated parameter values.

[Contact: Eric J. Vanzura, (303) 497-5752]

Williams, D.F., and Marks, R.B., **The Interpretation and Use of S-Parameters in Lossy Lines**, Conference Digest, 36th ARFTG Conference, Monterey, California, November 29-30, 1990, pp. 84-89 (1991).

Although a fundamental parameter of transmission lines, the characteristic impedance is difficult to measure accurately. We suggest a method by which it may be easily determined from a measurement of the propagation constant. The method is based on a rigorous analysis from first principles using explicit and realistic approximations which include the effects of imperfect conductors. Results of numerical studies of lossy coaxial lines and of experiments with coplanar waveguide indicate that high accuracy is possible.

[Contact: Dylan F. Williams, (303) 497-3138]

Williams, D.F., Marks, R.B., and Phillips, K.R., **Progress Toward MMIC On-Wafer Standards**, Conference Digest, 36th ARFTG Conference, Monterey, California, November 29-30, 1990, pp. 73-83 (1991).

A prototype standard set in coplanar waveguide suitable for the calibration of wafer probe stations has been developed through a cooperative effort between the National Institute of Standards and Technology and a MIMIC Phase 3 team. The coplanar standard set is intended primarily for in-process testing, although the characterization of coplanar waveguide circuits is also possible. In this paper, two sources of systematic errors associated with the prototype standard set, the propagation of undesirable modes, and the influence of adjacent structures on the electrical connection to the elements of the standard set are discussed.

[Contact: Dylan F. Williams, (303) 497-3138]

Released for Publication

Holt, D.R., **Determination of Scattering Parameters in Coaxial Air-Line Standards Using Self Consistency Conditions**, to be published as NIST Technical Note 1350.

Incident and reflected wave representations for voltage and current of the principal mode are developed for precision coaxial air line. The model allows for skin effect loss and dimensional variations of the inner and outer conductors. Expressions for the scattering parameters and characteristic impedance are found. Self-consistency conditions are employed to express the limitations of the model.

[Contact: Donald R. Holt, (303) 497-3574]

Judish, R.M., and Burns, J.G., **ARFTG Sponsors Measurement Comparison Program**.

The Automated Radio Frequency Techniques Group (ARFTG) has developed a program that provides ARFTG members the opportunity to compare the performance of their automatic network analyzers to that of their peers. This program is called the Measurement Comparison Program. Participants are provided an analysis of their measurement results in comparison to measurements made at other laboratories.

[Contact: Robert M. Judish, (303) 497-3380]

Reeve, G.R., **Millimeter Wave Metrology at the National Institute of Standards and Technology**, to be published in the Proceedings of the 1991 National Conference of Standards Laboratories Workshop and Symposium, Albuquerque, New Mexico, August 19-22, 1991.

Over the past several years, there has been an increased interest in the use of millimeter waves for such diverse applications as wide-band satellite communications, short-range radar and vehicle traffic control, and a much expanded cellular personal telephone service. Recent developments in gallium arsenide fabrication and MMIC devices promise low-cost, high-performance circuits. Over the past five years, the National Institute of Standards and Technology has been engaged in a program to expand its measurement services in this region of the spectrum. This paper describes the additions that have been made to these services and some of the technical challenges that were encountered during the process.

[Contact: Gerome R. Reeve, (303) 497-3557]

Williams, D.F., and Marks, R.B., **Approximate Determination of the Capacitance of Coplanar Lines**.

The capacitance and conductance per unit length of a transmission line are useful in the determination of its characteristic impedance, particularly with lossy transmission lines such as coplanar waveguide. The capacitance of coplanar lines is measured with two independent techniques. The results of both measurements agree closely with calculations. A technique for directly comparing the capacitance of two similar transmission lines is also demonstrated.

[Contact: Dylan F. Williams, (303) 497-3138]

Williams, D.F., and Marks, R.B., Relations Between the Scattering Parameters of Reciprocal Waveguide Junctions.

The Lorentz reciprocity condition is applied to junctions connected to uniform but otherwise arbitrary waveguides. Expressions relating the forward and reverse transmission coefficients are derived and separated into two terms, the first involving the phase of the reference impedance in the guide and the second, a new reciprocity factor. The usual condition equating the forward and reverse transmission coefficients is shown not to hold in the general case. Several examples are cited.

[Contact: Dylan F. Williams, (303) 497-3138]

Electromagnetic Properties

Recently Published

Estin, A.J., and Janezic, M.D., Improvements in Dielectric Measurements with a Resonant Cavity, IEEE Instrumentation and Measurement Technology Conference Record, Atlanta, Georgia, May 14-16, 1991, pp. 573-579 (1991).

This paper describes a technique for using the power of an automatic network analyzer to determine to very high accuracy the resonant frequency and intrinsic quality factor of a microwave resonant cavity. With this technique, measurement of complex permittivity of samples of dielectric material can be determined to new low levels of uncertainty.

[Contact: Michael D. Janezic, (303) 497-3656]

Janezic, M.D., and Grosvenor, J.H., Improved Technique for Measuring Permittivity of Thin Dielectrics with a Cylindrical Resonant Cavity, IEEE Instrumentation and Measurement Technology Conference Record, Atlanta, Georgia, May 14-16, 1991, pp. 580-584 (1991).

A new technique for measuring the permittivity of thin, low-loss dielectric materials in a cylindrical resonant cavity has been developed. A thin dielectric sample is placed upon a thicker dielectric sample whose permittivity is well characterized. Both samples are then placed on the endplate in the cylindrical resonant cavity. In this way, the thin sample is placed in a region of the cavity where interaction with the electromagnetic fields is greater. From knowledge of the cavity's resonant frequency, dimensions of the cavity and both dielectric samples, and the permittivity of the thicker sample, one is able to use iterative techniques to accurately determine the permittivity of the thin dielectric sample.

A derivation and discussion of the theory used in this layered-dielectric permittivity measurement technique is provided. Also, measurement results, at frequencies between 9 and 10 GHz, of thin cross-linked polystyrene, alumina, and magnesium titanate samples confirm that this measurement technique is able to accurately measure the dielectric constant of thin low-loss materials. A preliminary error analysis is also given to show the worst-case uncertainties associated with this new method.

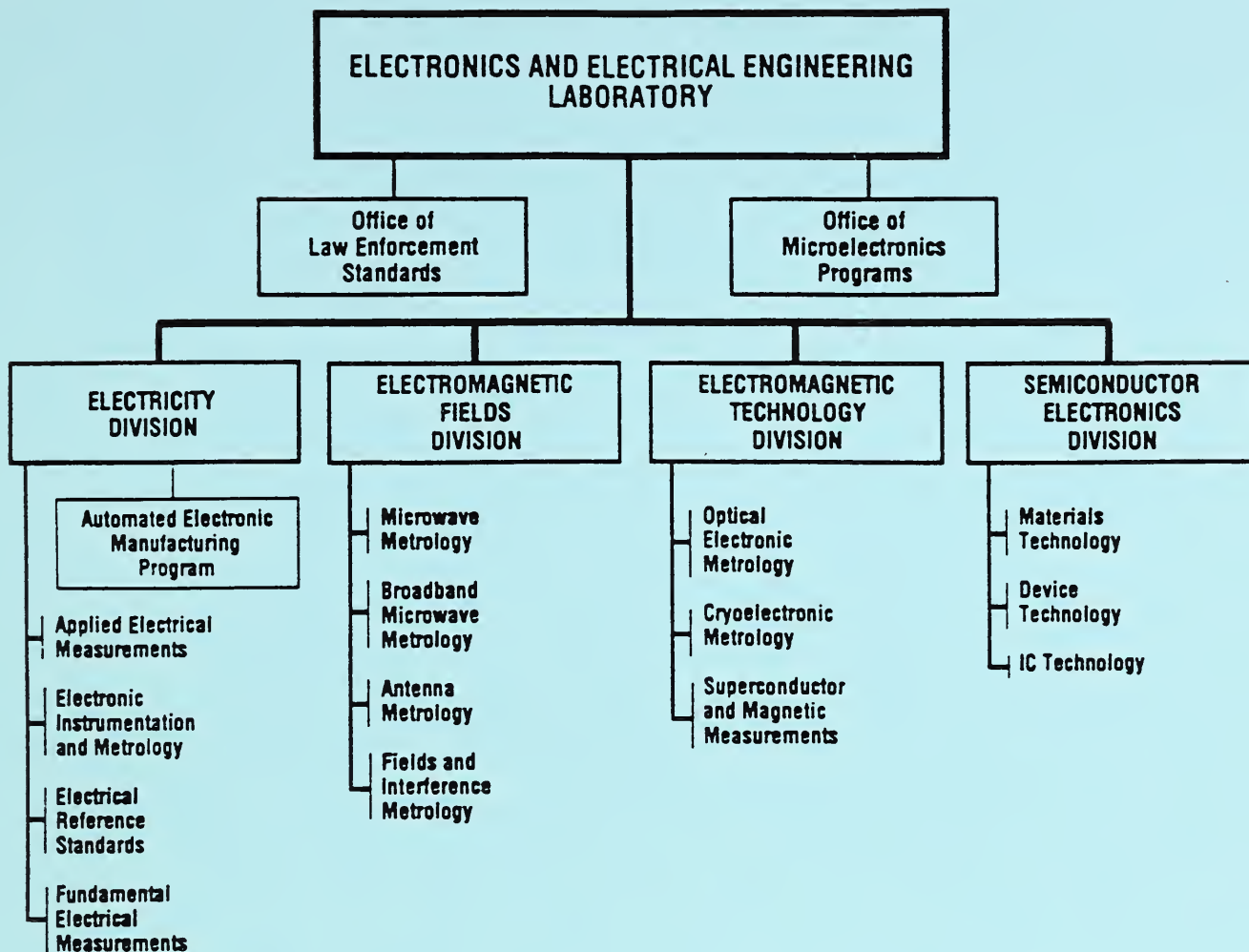
[Contact: Michael D. Janezic, (303) 497-3656]

Vanzura, E.J., and Rogers, J.E., Resonant Circuit Model Evaluation Using Reflected S-Parameter Data [original title: Evaluation of a Resonant Circuit Model Using Reflected S-Parameter Data], IEEE Instrumentation and Measurement Technology Conference, Atlanta, Georgia, May 14-16, 1991, pp. 150-155 (1991).

A nonlinear regression procedure is used to fit S-parameter resonance data to a full-circuit model that includes coupling factors and self-impedances. Such a model should provide an adequate mathematical representation of cavity resonator data. Our analysis shows that this model fits the data better than the simpler Q-circle model that can be derived from it, but that a systematic pattern in the residuals persists. This pattern indicates a discrepancy between the full-circuit model and the observed data. By looking at parameter estimates calculated from subsets of the original data, we demonstrate that the cause of this discrepancy could also be introducing significant errors in the model's estimated parameter values.

[Contact: Eric J. Vanzura, (303) 497-5752]

Weil, C.M., and Kissick, W.A., The NIST Electromagnetic Properties of Materials Program, IEEE Instrumentation and Measurement Technology Conference, Atlanta, Georgia, May 14-16, 1991, pp.



KEY CONTACTS

Laboratory Headquarters (810)	Director, Mr. Judson C. French (301) 975-2220
Office of Microelectronics Programs	Deputy Director, Dr. Robert E. Hebner (301) 975-2220
Office of Law Enforcement Standards	Director, Mr. Robert I. Scace (301) 975-4400
Electricity Division (811)	Director, Mr. Lawrence K. Eliason (301) 975-2757
Semiconductor Electronics Division (812)	Chief, Dr. Oskars Petersons (301) 975-2400
Electromagnetic Fields Division (813)	Chief, Mr. Frank F. Oettinger (301) 975-2054
Electromagnetic Technology Division (814)	Chief, Dr. Ramon C. Baird (303) 497-3131
	Chief, Dr. Robert A. Kamper (303) 497-3535

INFORMATION:

For additional information on the Electronics and Electrical Engineering Laboratory, write or call:
 Electronics and Electrical Engineering Laboratory
 National Institute of Standards and Technology
 Metrology Building, Room B-358
 Gaithersburg, MD 20899
 Telephone: (301) 975-2220

U.S. DEPARTMENT OF COMMERCE
NATIONAL INSTITUTE OF STANDARDS AND TECHNOLOGY
GAITHERSBURG, MD 20899

OFFICIAL BUSINESS
PENALTY FOR PRIVATE USE, \$300

BULK RATE
POSTAGE & FEES PAID
NIST
PERMIT No. G195